



This is the peer reviewed version of the following article: Eshaghzadeh, H., A. Akbarzadeh, M. Yarmohammadi, and E. Gisbert. 2018. "Skeletogenesis In The Persian Sturgeon Acipenser Persicus And Its Correlation With Gene Expression Of Vitamin K-Dependent Proteins During Larval Development". Journal Of Fish Biology 92 (2): 452-469. Wiley, which has been published in final form at <https://doi.org/10.1111/jfb.13527>. This article may be used for non-commercial purposes in accordance with Wiley Terms and Conditions for Use of Self-Archived Versions

21 **ABSTRACT**

22 The present study describes morphological development of the skeleton in the Persian
23 sturgeon *Acipenser persicus* Borodin 1897, and discusses the hypothesis that genes
24 encoding vitamin k-dependant proteins (VKDPs) might have a correlation with the
25 mineralization of skeletal tissues during early development in sturgeons. Results showed
26 that the development of cartilage started just after hatching (10.9 ± 0.7 mm in total
27 length, L_T) in the head and notochord, whereas the first signs of mineralization occurred
28 in the dentary and in the dermopalatine and palatopterygoid elements of the upper jaw,
29 coinciding with the onset of exogenous feeding (20.1 ± 1.5 mm L_T). All branchial arch
30 elements were developed between 19.3 and 22.3 mm L_T , whereas mineralization was
31 only observed in tooth plates associated with the hypobranchial 1 and gill rakers at 20.8
32 ± 1.5 mm L_T and 48.4 ± 6.4 mm L_T , respectively. Quantitative real-time PCR showed
33 that transcripts of VKDP genes including bone Gla protein (*bgp*), matrix Gla protein
34 (*mgp*) and Gla rich protein (*grp*) were significantly up-regulated during the transition to
35 exogenous feeding, supporting hypotheses about relevance of the above-mentioned
36 genes in chondrogenesis at early developmental stages. The strong mineralization of
37 skeletal elements from 21.5 – 27.3 mm L_T (20 dph) was in accordance with the maximal
38 levels of *bgp*, *mgp* and *grp* expression indicating a correlation between development of
39 the skeleton and the expression of VKDP genes. This information may be considered as
40 a reference for future studies evaluating the quality of larvae and the influence of rearing
41 biotic and abiotic factors on skeletogenesis and the occurrence of skeletal deformities in
42 this species.

43 Key words: development, gene expression, skeleton, vitamin k-dependant proteins.

44

45

46

INTRODUCTION

47 The fish skeletal system provides mechanical support to soft tissues and levers for
48 muscle action, providing greater efficiency for locomotion, among other functions such
49 as the mobilization or deposition of calcium and phosphorus which contributes to
50 calcium homeostasis (Boglione *et al.*, 2013a). Skeletogenesis is therefore important not
51 only for understanding changes in swimming behaviour (Osse & Van den Boogart,
52 1995), but also for evaluating the quality of hatchery-produced fish (Boglione *et al.*,
53 2013a, b). Skeletal abnormalities mostly appear during larval and early juvenile stages,
54 when the skeleton differentiates and achieves its definitive configuration (Boglione *et*
55 *al.*, 2013a). Many factors such as physiological, environmental, genetic, xenobiotic and
56 nutritional can affect this process (Boglione *et al.*, 2013b); therefore, analysis of the
57 skeletal system at early stages of development is an useful tool for assessing rearing
58 conditions (i.e. environmental and nutritional) and their quality, regardless of whether
59 fish are to be used for stocking or food production. Skeletogenesis must also be
60 understood to understand the expression of skeleton-associated genes and proteins
61 (Gavaia *et al.*, 2006; Fernández *et al.*, 2011). The formation of bones and other
62 cartilaginous and mineralized tissues in fishes depends upon the expression of a wide
63 variety of genes (Boglione *et al.* 2013a). This study examines a particular group of
64 genes coding for vitamin k-dependant proteins (VKDPs), also known as γ -
65 carboxyglutamic acid (Gla) proteins, including bone Gla protein (BGP), matrix Gla
66 protein (MGP) and Gla rich protein (GRP) (see review in Dourado-Villa *et al.*, 2017).

67 These proteins belong to the family of Ca²⁺-binding vitamin K-dependent proteins and
68 are recognized by having several Gla residues that are converted from the post-
69 translation modifications of specific glutamates (Glu) via the γ -glutamyl carboxylase
70 enzyme (GGCX) (Vermeer, 1990; Viegas *et al.*, 2008). Both BGP (osteocalcin) and
71 MGP are important in the regulation of mineral deposition in calcified tissues
72 (Hashimoto *et al.*, 2001; Viegas *et al.*, 2013). BGP is synthesized by osteoblasts and
73 odontoblasts and functions as a regulator of bone maturation (Boskey *et al.*, 1998;
74 Krossøy *et al.*, 2009). MGP is also synthesized by osteoblasts but, in contrast to BGP, it
75 is also synthesized by a wide variety of other cells, like vascular smooth muscle cells
76 and chondrocytes (Krossøy *et al.*, 2009). MGP is believed to be more important for
77 regulating mineral deposition in vascular system and cartilage and it has a minor role in
78 the regulation of chondrocyte maturation (Luo *et al.*, 1997). GRP may also directly
79 influence mineral formation, thereby playing a role in processes involving connective
80 tissue mineralization (Viegas *et al.*, 2009). In the skeleton, most relevant levels of *grp*
81 gene expression have been observed in cartilaginous tissues and associated with
82 chondrocytes and chordoblasts (Viegas *et al.*, 2009; Cancela *et al.*, 2012), suggesting a
83 role in chondrogenesis. However, *grp* expression has also been detected in bone cells,
84 which is indicative of a more widespread role for the protein throughout skeletal
85 formation (Cancela *et al.*, 2012; Dourado-Villa *et al.*, 2017). Previous studies in teleosts
86 have revealed an increase in expression of both *bgp* and *mgp* genes, paralleling
87 calcification of axial skeleton structures during larval development (Gavaia *et al.*, 2006).
88 Despite the potential role of VKDPs in soft tissue mineralization and bone formation,
89 little is known about the expression of genes encoding VKDPs (*i.e.* *mgp*, *bgp* and *grp*)

90 during sturgeon larval development. However, it has been found that the expression of
91 *bgp*, *mgp* and *grp* genes in cartilaginous and bony tissues occurs in higher levels in adult
92 sturgeons compared to mammals (Viegas *et al.*, 2008; Viegas *et al.*, 2013) and teleosts
93 (Krossøy *et al.*, 2009).

94 Continuous drastic declines in natural sturgeon populations over the past 30
95 years plus a high market demand for caviar have led the way for sturgeon farming,
96 mainly for the production of caviar. According to Bronzi *et al.* (2011), the caviar output
97 from aquaculture was 260 t in 2012, a production that was estimated to increase up to
98 500–750 t within the next 10 years. Sturgeons belong to the order Acipenseriformes
99 (infraclass Chondrostei) and can provide useful information about mechanisms involved
100 in the evolution of vertebrates, especially teleost fishes (Viegas *et al.*, 2013).
101 Acipenseriformes diverged from the lineage leading to teleosts during the Devonian Age
102 of Fishes (~385 million years ago) (Near *et al.*, 2012) and in contrast to teleosts, they
103 have retained a dermal skeleton (Jollie, 1980; Grande & Hilton, 2006; Hilton *et al.*,
104 2011). As Leprévost & Sire (2014) reviewed, few morphological studies on the skeleton
105 of Acipenseriformes are available, even though a renewed interest in sturgeon biology
106 has recently been promoted by their commercial importance, uniqueness and almost
107 universally endangered status (Findeis, 1997). This information is incomplete and
108 fragmented in terms of species, and also in terms of age; in particular, out of the 25
109 living acipenserid species, the skeleton of only 13 species and a hybrid has been studied,
110 and the axial skeleton is often not the main topic of such studies (Leprévost & Sire,
111 2014). Considering the unique properties of the skeleton in Acipenseriformes, including
112 an internal cartilaginous skeleton, five rows of bony plates, ganoid scales on the body

113 surface, and lack of a vertebral centrum (Viegas *et al.*, 2008; Viegas *et al.*, 2010),
114 coupled with their distinctive skeletogenesis, it is worth investigating normal patterns of
115 skeletal development, which will be essential to accurately assess deformities in
116 hatchery-produced fry, detect critical stages during skeletogenesis and improve actual
117 larval rearing practices in this commercially important and endangered group. Thus, the
118 objectives of the present study were to describe the ontogenetic development of the
119 skeleton of hatchery-reared Persian sturgeon (*Acipenser persicus* Borodin 1897), as
120 well as to evaluate changes in the expression of genes encoding for VKDPs including
121 *bgp*, *mgp* and *grp*, which are known to be involved in the formation and mineralization
122 of skeletal tissue.

123

124

125 MATERIAL AND METHODS

126

127 ANIMALS AND SAMPLING PROTOCOL

128 Specimens of *A. persicus* were obtained from broodstock held at the Shahid Beheshti
129 Artificial Sturgeon Propagation and Rearing Center (Rasht, Iran). Six adult individuals
130 (two males and four females) were induced to spawn and spermiate with an
131 intramuscular injection of LHRH-A2 hormone (3 $\mu\text{g kg}^{-1}$ body weight). Egg
132 adhesiveness was removed by a 45-min treatment with a clay-water suspension;
133 fertilised eggs were transferred to 15-L Yoshchenko incubators (500 g eggs per
134 incubator) connected to an open-flow freshwater system. During the egg incubation
135 period, water temperature was 14.4 °C and progressively increased up to 17.4 °C;

136 prelarvae hatched seven days after fertilization. At hatching, prelarvae were transferred
137 to three 500-L circular fiberglass tanks with water depth of 30 cm, and initial density of
138 10 larvae L⁻¹ (10 g prelarvae per tank). *Artemia* nauplii were administered to larvae from
139 eight days post hatching (dph) (150·2 degree days post hatching, ddph) to 12 dph (237·2
140 ddph) five times per day; after which larvae were fed with a mixture of cladocerans
141 (*Daphnia* sp.) and *Artemia* metanauplii from 12 to 50 dph. Samples were taken at 10
142 different times: at hatching (0), 1, 3, 6, 10, 12, 14, 20, 30 and 50 dph. Fish were
143 euthanized by an overdose of tricaine methanesulfonate (MS-222, Argent, Chemistry
144 Laboratories, Redmond, USA), with 10 individuals immediately deep-frozen in liquid
145 nitrogen and stored at -80 °C until RNA extraction. Ten additional individuals from the
146 above-mentioned time-points were also fixed in 4% buffered formalin for descriptive
147 purposes.

148 During fish rearing, water temperature, dissolved oxygen and pH levels were
149 14·2 ± 0·9 °C, 7·9 ± 1·2 mg l⁻¹ and 7·4 ± 0·5, respectively. Photoperiod was 12L: 12D,
150 and light intensity 200 lux at the water surface. Before fixation, the left side of each
151 specimen was photographed using a Cannon camera (EOS 20D, 8 MP resolution)
152 coupled to a stereomicroscope (EP600, Nikon, Japan), and total length (L_T) measured to
153 the nearest mm using ImageJ (version 1·240). Yolk sac volume was determined
154 according to Eshaghzadeh *et al.* (2017). Developmental stages of *A. persicus* were
155 designated as prelarva, larva and early juvenile according to Dettlaff *et al.* (1993). The
156 experimental work and fish procedures were carried out according to the requirements
157 of The Iranian Society for The Prevention of Cruelty to Animals.

158

159 *STAINING OF THE SKELETON*

160 In order to describe the process of skeletogenesis in *A. persicus*, fish were stained
161 according to Hanken & Wassersug (1981). Briefly, samples were transferred into 100%
162 ethanol, rehydrated in gradually decreasing ethanol series (75, 50, and 25 %), and
163 washed with distilled water. Fish were incubated in Alcian blue (AB) solution (10 mg
164 Alcian blue 8GX, SIGMA A5268 in 70 ml absolute alcohol and 30 ml acetic acid).
165 Larvae were then incubated in a trypsin solution (1 g trypsin in 30% saturated borax
166 solution dissolved in 70 ml distilled water) for 2-8 hours depending on fish size. For
167 mineralized elements staining, specimens were transferred into a staining solution
168 containing 0.5% KOH and Alizarin red S (SIGMA T4799). Finally, fish were washed
169 with distilled water and then incubated in the gradually increasing series of glycerol +
170 1% KOH (25%, 50%, 75%, and pure glycerol) for clearing and complete elimination of
171 the nonspecific staining of soft tissues. Staining of cartilaginous skeletal structures by
172 Alcian blue solution at low pH values (pH = 2.0) did not result in important staining
173 skeletal artifacts [poor staining of mineralized elements, which are few in the skeleton of
174 Acipenseriformes (Hilton *et al.*, 2011; Lprevost & Sire, 2014)], since mineralized
175 elements were not decalcified during the cartilage staining step. Thus, the acid double
176 staining protocol used in this study (Hanken & Wasserug, 1981) was compared with the
177 acid-free staining protocol from Walker and Kimmel (2007) in early juveniles aged 50
178 dph (Figure 1).

179 *TOTAL RNA EXTRACTION AND COMPLEMENTARY DNA SYNTHESIS*

180 Total RNA was extracted from three separate individuals (biological replicates) using
181 Biozol Reagent (Bioflux-Bioer, China) and treated with DNase I (Fermentas, France)

182 according to the manufacturer's instructions. The integrity of RNA was evaluated in a
183 1.5 % agarose electrophoresis gel and RNA quantity was determined by a NanoDrop
184 ND-1000 Spectrophotometer (Thermo Scientific, Wilmington, DE, USA). All RNA
185 samples had 260/280 ratios of 1.8-2.0 and 260/230 values of 2.0-2.2. One microgram of
186 total RNA was used to synthesize first-strand cDNAs using a MMuLV reverse transcriptase
187 and 2.5 µM oligo-dT following the manufacturer's instructions (Fermentas, France).

188

189 *PRIMER DESIGN AND QUANTITATIVE REAL-TIME PCR (qPCR)*

190 The qPCR primers for *bgp* and *grp* were designed based on sequences available in
191 GenBank (accession numbers: EF413584, EU482149.1) from Adriatic sturgeon (*A.*
192 *nacarii*) (Viegas *et al.*, 2008). Regarding *mgp*, primers were designed considering the
193 sequence for *A. nacarii* (accession number: HM182000.1) and from two Teleostei
194 species: turbot (*Scophthalmus maximus* (Linnaeus 1758)) and gilthead seabream (*Sparus*
195 *aurata* (Linnaeus 1758)) (accession numbers: DQ304476.1, AY065652.1). qPCR
196 primers were designed for each gene using Primer3 (Table 1) and the specificity and
197 size of the amplicons obtained with primer pairs were checked on a 1.5% agarose gel.
198 The fragments were sequenced using the ABI 3130 Genetic Analyzer (Applied
199 Biosystems, USA). Chromatograms were checked and sequences manually aligned
200 using the program BioEdit software Version 5. Identities of the sequences were verified
201 by BLAST (<http://ncbi.nlm.nih.gov/BLAST>). Sequences obtained for *bgp*, *grp*, and *mgp*
202 in *A. persicus* were submitted to GenBank (accession numbers: MF687668, MF687669
203 and MF687670, respectively). Primers for ribosomal protein L6 (*rpl6*) and β-actin

204 (*actb*), and their geometric average of messenger RNA (mRNA) level were used for the
205 standardization of expression levels (Akbarzadeh *et al.*, 2011).

206 Quantitative real-time PCR (qRT-PCR) was run on a CFX96 Real-Time PCR
207 Detection System (Bio-Rad, USA), using the CFX manager 1.6 software (Bio-Rad) and
208 the following PCR protocol: pre-denaturation at 94 °C for 1 min, 40 cycles of
209 denaturation at 94 °C for 15 s, annealing at 60 °C for 15 s, and extension at 72 °C for 30
210 s. Each reaction was performed using a total volume of 12 µl solution, with 1 x SYBR
211 Green Bio-Easy mastermix (Bioer-Bioflux), 2.5 µM of ROX reference dye, 100 nM of
212 each primer with 2 µl of cDNA template. Baseline, threshold (for Ct calculation),
213 melting curve analysis (for verify the specificity of the target and absence of primer
214 dimers) and standard curves (for PCR efficiency) among samples were determined as
215 described in Akbarzadeh *et al.* (2011). Prior to statistical analysis, an amplification
216 efficiency (E) was determined for each target gene as $E\% = (10^{1/\text{slope}} - 1) \times 100$, where
217 the slope was estimated plotting the Ct in a serial dilutions of cDNA. Amplification
218 efficiencies for all target and reference genes ranged between 91 to 99%. The mRNA
219 expression of target genes (*bgp*, *mgp*, *grp*) relative to the reference genes (*actb* and *rpl6*)
220 was calculated by the $2^{-\Delta\Delta Ct}$ method (Livak & Schmittgen, 2001). Among the
221 developmental time-points, the sample at 1 dph was chosen as the reference sample to
222 evaluate the differential mRNA expression of target genes.

223

224 STATISTICS

225 All qRT-PCR data were log-transformed and the homogeneity of variances and
226 normality were assessed by Bartlett's and Kolmogorov–Smirnov tests, respectively.

227 Differences in gene expression data between different developmental time-points were
228 analyzed by a one-way analysis of variance (ANOVA), followed by a Tukey's HSD
229 *post hoc* analysis for multiple comparisons. Differences were considered statistically
230 significant at $P < 0.05$. SPSS (version 19.0) was used for statistical analysis.

231

232

233

RESULTS

234

MORPHOLOGICAL DEVELOPMENT AND SKELETOGENESIS

235 At hatching, prelarvae measured 10.9 ± 0.7 mm in L_T and weighed 19.6 ± 0.3 mg in
236 body weight (BW), showing a large yolk-sac (17.2 ± 4.4 mm³). The posterior part of the
237 body was surrounded by a wide primordial finfold, and no mineralized skeletal
238 structures were visible (Figure 1a). Microscopic observations showed that sensory
239 organs such as olfactory, gustatory and vision were not developed when prelarvae
240 emerged from egg envelopes. At one dph (12.3 ± 0.9 mm L_T), the mouth and gill
241 openings were cleaved with four branchial arches (AB-negative, but visible by
242 transparency through the opercular region), pigmented eyes and barbel buds were also
243 visible, and rudiments of the pectoral fin appeared like distinct folds. The head began to
244 straighten and cartilaginous skeletal pieces started to stain with AB (Figure 1b). At three
245 dph (14.1 ± 0.5 mm L_T), the finfold was wider on the ventral side of the trunk, narrowed
246 at the caudal peduncle, and protruded slightly in the region where the future dorsal,
247 caudal and anal fins will develop, the melanin plug (accumulation of melanin residues
248 derived from yolk sac consumption) was visible in the anterior intestine, eyes were
249

250 darkly pigmented, the paired and single fins in the tail and trunk were still invisible.
251 Lower and upper lips were covered by small folds around the buccal cavity, and the
252 Meckel's and palatoquadrate cartilages appeared in the mandible and maxillary areas,
253 respectively (Figure 1c). At six dph (17.3 ± 0.8 mm L_T), the size of barbels increased
254 and the branchial cavity showed that external gills were not completely covered by the
255 operculum yet. Olfactory holes were joined to each other by olfactory lobes, yolk sac
256 was divided into two unequal parts and most of the yolk-sac was consumed, showing a
257 reduction in volume of about 76.2 % (Fig. 1d).

258 At 10 dph (19.9 ± 1.7 mm L_T), the dorsal fin was distinguishable from the
259 bordered margin of the posterior part of primordial finfold, teeth were already detected
260 in both jaws, but they were not mineralized (Figure 2a), and the rudiments of dorsal
261 scutes ($n = 9-11$) were observed stained in Alcian blue in the dorsal part of the finfold.
262 Branchiostegals were clearly visible in the splanchnocranium, and gill arches were
263 completely formed. Several unmineralized structures, such as two basibranchial copulae,
264 three hypobranchials and five ceratobranchials were visible on the ventral portion of the
265 branchial arches at 10 dph (Figure 2d). Also, un-mineralized hyoid arches including the
266 hyomandibular, interhyal, hypohyal, and posterior and anterior ceratohyals were clearly
267 distinguished (results not shown). Cartilaginous elements of the subopercle, cleithrum
268 and postcleithrum appeared in the posterior margin of the head. In the hyoid arch, the
269 posterior end of the interhyal was linked to the ventral part of hyomandibular and
270 posterior ceratohyal, whereas the anterior end of the interhyal was connected to the
271 posterior portion of the lower jaw (palatoquadrate). At this age and body size, there still
272 seemed to be no mineralized elements in the skeleton of *A. persicus* (Figure 1e).

273 The first identified element to mineralize was the dentary, and also in the
274 dermopalatine and palatopterygoid elements of the upper jaw at 12 dph (20.1 ± 1.5 mm
275 L_T), coinciding with the onset of exogenous feeding. External gills were largely covered
276 by the extended operculum, and teeth were observed arranged in a row on the dentary
277 and dermopalatine mineralized elements, whereas two irregular rows of teeth were
278 visible on the palatopterygoid mineralized element (Figure 2b). Between six and 12 dph,
279 the formation of pelvic, anal and caudal fins was clearly distinguishable, whereas the
280 dorsal fin had between 15 to 19 pterygiophores of the distal radials, middle radials and
281 proximal radials, and five to seven metapterygial radials appeared in the pectoral fin.
282 Unmineralized pterygiophores in the anal fin and between 22 to 26 unmineralized
283 hypurals in the caudal fin were observed between 12 and 14 dph (20.8 ± 1.5 mm L_T).
284 Hypurals developed on the anteriormost end of the caudal fin, forming its heterocercal
285 structure (Figure 1f, g, j). No major changes in the formation of the skull were detected
286 between 14 and 20 dph. Different mineralized skeletal elements from the cephalic
287 region such as the subopercle, supracleithrum and parietal were found weakly
288 mineralized at 20 dph (24.4 ± 2.9 mm L_T) (Figure 1h, 2c).

289 At 30 dph (33.4 ± 3.8 mm L_T), *A. persicus* specimens had a similar appearance
290 to small juveniles and adults. At this age, the snout elongated and all morphological
291 structures were totally developed and some new juvenile traits appeared such as five
292 longitudinal rows of bony scutes, a ventrally-flattened body, elongated barbels, a
293 completely differentiated heterocercal caudal fin composed of the basidorsals,
294 basiventrals, distal radial, hypurals, supraneural and fin rays, and teeth on upper and
295 lower jaw missing. Cartilaginous elements of the pelvic pterygiophores were observed at

296 30 dph (Figure 1i). Mineralization of the lateral row of scutes, cleithrum and rostral
297 canal bones had already began at this age, while mineralization just started and
298 continued to increase in the pectoral-fin spine, frontal, dermopterotic, jugal and
299 dermosphenotic elements (Fig 1i). Finally, the last mineralized elements to form
300 between 30 and 50 dph (48.4 ± 6.4 mm L_T ; Fig 2e, f, g and 1j) were the parasphenoid,
301 nasal, ventral and dorsal rostral elements, postorbital and median extrascapular bones, as
302 well as two series of ventral scute rows ($n = 12-13$ per row) where the posteriormost
303 ventral scute of two scute series contact each other just after the anal fins. During this
304 period, teeth on the mineralized dentary, dermopalatine and palatopterygoid elements
305 disappeared.

306

307 *DEVELOPMENTAL EXPRESSION OF VKDPs CODING GENES*

308 Transcripts of *bgp*, *mgp* and *grp* were detected in all developmental time-points of *A.*
309 *persicus* from one to 50 dph. Changes in *bgp* expression levels changed over
310 development ($P < 0.05$). As shown in Figure 3a, expression of *bgp* in *A. persicus*
311 significantly increased from the onset of exogenous feeding at 10 dph to the early
312 juvenile stage at 50 dph. The highest expression of *bgp* was observed at 30 dph when *A.*
313 *persicus* resembled small juveniles.

314 Figure 3b illustrates changes in the expression levels of *mgp* during early
315 development in *A. persicus*. Expression of *mgp* changed during prelarval, larval and
316 early juvenile stages ($P < 0.05$). Transcript levels of *mgp* followed a similar trend to that
317 observed in *bgp* expression; specifically, *mgp* expression did not significantly vary

318 during the prelarval stage ($P > 0.05$), whereas it significantly increased coinciding with
319 the beginning of exogenous feeding and progressively increased until the early juvenile
320 stage at 50 dph, although relative levels of *mgp* transcripts decreased at 30 dph ($P <$
321 0.05), reaching similar values to those observed during the prelarval and larval stages,
322 but increased again before the end of the study at 50 dph (Figure 3b).

323 Levels of *grp* transcripts showed a moderately increasing trend from one to 20
324 dph, except for 14 dph, although this trend was not statistically significant ($P > 0.05$).
325 At 30 dph the *grp* expression reached maximal value, whereas at 50 dph, *grp* values
326 decreased and were similar to those observed at younger ages (one to six dph) (Figure
327 3c).

328

329

DISCUSSION

330 Osteological studies are a very useful tool for understanding the functional demands and
331 environmental needs of an organism during different stages of development (Boglione *et*
332 *al.*, 2013a, b). According to the present study, the skeletal development of *A. persicus*
333 could be divided into three main stages: 1) from hatching to the start of exogenous
334 feeding (prelarval stage), during which cartilage elements of the skull with crucial roles
335 in feeding and respiratory activity were formed but no mineralization occurred; 2) from
336 the onset of exogenous feeding to the complete absorption of yolk sac reserves (mixed
337 nutrition period), during which first mineralization processes and development of
338 chondrogenesis related to feeding, swimming and respiratory activity occurred in larvae;
339 and 3) from the end of the mixed nutrition period to the early juvenile period, which was

340 characterized by the development of all other mineralized elements of the skull roof
341 (neurocranium), mineralization of bony scutes (dorsal, lateral and ventral in
342 chronological order), appearance of the rostral sensory bone, and complete
343 mineralization of cartilage elements that appeared at earlier stages.

344 The correct evaluation of mineralization is fundamental for the study of skeletal
345 development maintenance, and regeneration (Bensimon-Brito *et al.*, 2016). Some
346 authors have reported that decalcification may occur in skeletal elements of teleost fish
347 larvae, which are often only a few millimeters long, because of the use of acetic acid in
348 the AB dye that may slightly demineralise skeletal elements and therefore lose their
349 affinity for Alizarin red dye (Gavaia *et al.*, 2000). Traditionally, cartilage is stained by
350 AB blue using acidic conditions to differentiate tissue staining; however, the acidic
351 conditions may be problematic when one wishes to stain the same specimen for
352 mineralized bone with Alizarin red, because acid demineralizes bone by dissolving
353 hydroxyapatite, which negatively affects bone staining (Walker & Kimmel, 2009). Data
354 from this study with regard to the chronological development of small skeletal elements
355 (*e.g.* dermopalatine, palatopterygoid, dentary, subopercle, supracleithrum, posttemporal
356 and parietal) should be taken with caution since it is not possible to determine whether
357 some demineralisation occurred in these elements due to the use of an acidic protocol
358 double staining of skeletal structures (Walker & Kimmel, 2009). However, in the case of
359 sturgeon larvae that are generally *ca.* five to 10 times larger than teleost larvae, we did
360 not observe a remarkable loss of staining affinity to Alizarin red of skeletal elements,
361 when using either acidic (Hanken & Wasserug, 1981) or non-acid (Walker and Kimmel,
362 2007) staining protocols, especially in dermal scute rows that were strongly stained in

363 red as soon as they were visible under the dissecting microscope. These differences
364 between acipenserids and teleosts may be due to the larger size of sturgeon larvae in
365 comparison to teleosts, as well as different staining-times employed between these fish
366 groups. In this study, it took 30–60 min to stain sturgeon larvae of 10–24 mm, while for
367 smaller marine teleost larvae (3–4 mm) at the same developmental stage staining time is
368 shorter (10–15 min) (Gavaia *et al.*, 2000).

369 *SKELETAL DEVELOPMENT*

370 According to the obtained results, no cartilaginous or mineralized elements were
371 observed in the skull of *A. persicus* at hatching, whereas the notochord was the main
372 skeletal element distinguishable at this stage. The lack of vertebral centra and the
373 presence of a persistent notochord are considered as common features of the axial
374 skeleton in the early ontogeny of sturgeons (Hilton *et al.*, 2011; Leprévost & Sire,
375 2014). The notochord is a medial structure that appears early in the embryo of all
376 vertebrates, and has several important functions in biochemical and physiological
377 signaling (Wang *et al.*, 2014). In agreement with previous studies, the axial skeleton of
378 *A. persicus* differs from that of teleost species. It is composed of a notochord,
379 basidorsals, basiventrals, interdorsals, interventrals, neural spines, and ribs as in other
380 sturgeon species (Hilton *et al.*, 2011; Zhang *et al.*, 2012; Leprévost & Sire, 2014). In *A.*
381 *persicus*, the first mineralized bones, the dermopalatine, palatopterygoid and dentary
382 were observed between 18.6–21.6 mm L_T (12 dph). Mineralization of teeth and the
383 complete covering of the external gills by the operculum, which might enhance prey
384 seizure and gill development, respectively (Gisbert, 1999; Park *et al.*, 2013;
385 Eshaghzadeh *et al.*, 2017), are considered to be the most important events in the

386 development of the larval sturgeon splachnocranium, These changes were concomitant
387 with the onset of exogenous feeding, the complete differentiation of the digestive organs
388 and increase in digestive enzyme activities relative to earlier stages of development
389 (Babaei *et al.*, 2011), which might be indicative of growth priorities during early
390 development, which allometric growth studies have revealed in this group of fishes
391 (Gisbert, 1999; Gisbert & Doroshov, 2006; Gisbert *et al.*, 2014; Eshaghzadeh *et al.*,
392 2017). In addition, the presence of unmineralized teeth and mineralized dentary and
393 dermopalatine elements in *A. persicus* prelarvae just before the onset of exogenous
394 feeding was in agreement with descriptions in shortnose sturgeon (*A. brevirostrum*
395 Lesueur, 1818) (Hilton *et al.*, 2011) and Siberian sturgeon (*A. baerii* Brandt, 1869) (Park
396 *et al.*, 2013). Between 21.5 and 37.2 mm L_T (20 and 30 dph), mineralization was
397 observed in the following skeletal elements: the subopercle, supracleithrum,
398 posttemporal, parietal and the dorsal scute row. These results are in contrast with those
399 obtained in teleost fishes, which showed earlier mineralization in the above-mentioned
400 cranial structures (Gluckmann *et al.*, 1999; Wagemans & Vandewalle, 2001). In this
401 study, the initial formation of dorsal, lateral and ventral rudimentary scute rows took
402 place asynchronously with regard to age and fell within the values reported for other
403 acipenserid species. In particular, the initial formation and mineralization of dorsal
404 scutes in *A. brevirostrum* were detected between 20.5 to 21.9 mm L_T (Hilton *et al.*,
405 2011), whereas these occurred between 19.7 to 21.0 mm L_T (Gisbert, 1999), and 20.6 to
406 26.0 mm L_T (Park *et al.*, 2013) in *A. baerii*, although no specific methods using double-
407 staining techniques were used for evaluating the development and mineralization of
408 skeletal structures in either study of *A. baerii*. Similar to other sturgeon species, the

409 order of mineralization of scute rows in *A. persicus* began with the dorsal followed by
410 the lateral and then ended with the ventral row (Hilton *et al.*, 2011; Park *et al.*, 2013;
411 Gisbert *et al.*, 2014; Eshaghzadeh *et al.*, 2017), although there existed some species-
412 specific variations in the sequence of scute formation and mineralization, which might
413 be related to many factors including different growth rates, availability of dietary
414 minerals, and different rearing conditions as has been postulated (Khajepour &
415 Hosseini, 2010; Park *et al.*, 2013).

416 The chronological order of formation of the neurocranial dermal skeleton in *A.*
417 *persicus* was characterized by initial development of the parietal mineralized elements
418 followed by the frontal and parasphenoid between 20 and 30 dph. Similarly, in *A.*
419 *brevirostrum*, the first signs of mineralization in the neurocranium were observed in
420 both parietals (Hilton, 2005; Hilton *et al.*, 2011). Several structures of the
421 splanchnocranium, such as the Meckel's cartilage, pars autopalatina, hyoid arch,
422 dermopalatine and dentary, were differentiated just before the onset of exogenous
423 feeding in *A. persicus*, likely due to the important role they play in protractile-mouth-
424 type suction feeding behavior that is typical of sturgeons (Wagemans & Vandewalle,
425 2001). As Hilton *et al.* (2011) described, elements of upper and lower jaws are fused to
426 each other through the hyoid arches, and mandibular elements are not joined to the
427 neurocranium in sturgeon species. Moreover, the hyomandibular is inserted directly
428 between the neurocranium and opercular elements. In *A. persicus*, suspensorium
429 elements were developed simultaneously at 18.2–21.6 mm L_T (10 dph), but no
430 mineralized elements were observed before the end of the study. However, in older
431 specimens of *A. brevirostrum*, some parts of the hyoid arch such as the hyomandibular,

432 the interhyal and the anterior ceratohyal were completely mineralized (Hilton, 2005;
433 Hilton *et al.*, 2011). Mineralization of suspensorium elements developed gradually and
434 jaw protrusion coincided with the loss of temporary teeth and a shift in the type of
435 feeding from prey seizure to suction feeding by creating negative pressure in buccal
436 cavity (Gisbert & Doroshov, 2003). Different mineralization patterns have been
437 observed in the branchial arches of acanthopterygians (Wagemans & Vandewalle,
438 2001). In *A. persicus*, all of the branchial arch elements were completely developed
439 between 19.3 and 22.3 mm L_T (14 dph), whereas mineralization was only observed in
440 teeth plates associated with hypobranchial 1 and gill rakers at 20.8 ± 1.5 mm L_T (14
441 dph) and 48.4 ± 6.4 mm L_T (50 dph), respectively. Differences in the time of
442 mineralization in branchial arch elements are likely related to feeding type (suction
443 feeding), the late transition from cutaneous to gill respiration in comparison to the
444 teleost larvae, the increasing nutritional demands associated with suction feeding and the
445 methodology used for bone and cartilage staining (Wagemans & Vandewalle, 2001;
446 Boglione *et al.*, 2013a).

447 After the development of mineralized and cartilage elements related to feeding
448 and respiratory systems, which occurred between 19.9 ± 1.7 and 20.1 ± 1.5 mm L_T (10
449 and 12 dph), the next priority in terms of osteological development in *A. persicus* larvae
450 was the development of skeletal elements needed for supporting unpaired and paired
451 fins. The first fins to form in chronological order were the pectoral fins, followed by the
452 dorsal, anal and caudal fins, with pelvic fins being the last ones to form. Formation of
453 the pectoral girdle was concomitant with the onset of exogenous feeding, which may be
454 linked to the need for pectoral fins to assist with orienting the mouth over prey,

455 correcting head yaw (Osse *et al.*, 1995), promoting body roll, and affecting changes in
456 vertical body position during maneuvering as described by Wilga & Lauder (1999). A
457 similar sequence of fin formation was shown in bony fish (Sfakianakis *et al.*, 2004) and
458 sturgeons (Hilton *et al.*, 2011).

459

460 *EXPRESSION OF VKDPs CODING GENES*

461 In the present study, the mRNA levels of genes encoding extracellular matrix proteins
462 (*bgp*, *mgp* and *grp*) were up-regulated from 10 dph, at the time when *A. persicus* larvae
463 started exogenous feeding. Regardless of the fact that these genes are not only expressed
464 in skeletal structures (Dourado-Villa *et al.*, 2017), the up-regulation of genes encoding
465 *bgp*, *mgp* and *grp* in *A. persicus* was consistent with initial mineralization and
466 chondrogenesis processes related to feeding, swimming and respiratory systems. These
467 results suggest that bone and cartilage-related Gla proteins play a role in skeletal
468 mineralization in sturgeons, if translation efficiency is not affected and translation
469 occurred consistent with mRNA expression. The biological importance of the increasing
470 trend in *mgp*, *bgp* and *grp* expression observed in this study could be related to the need
471 for more efficient mechanisms to control mineralization, and development of organs and
472 systems needed to meet the functional demands of the developing larvae (Gavaia *et al.*,
473 2006; Wang *et al.*, 2014). Comparison of the results obtained from this study and
474 available data from higher vertebrates (Gavaia *et al.*, 2006; Viegas *et al.*, 2013),
475 strengthen the hypothesis of a conserved function for Gla proteins from
476 Acipenseriformes to humans, which span more than 450 million years of evolution.

477 The mRNA expression of *bgp* increased from the onset of exogenous feeding to
478 the end of the study. The *bgp* protein is produced by osteoblasts in elements undergoing
479 mineralization and odontoblasts during skeletogenesis (Pinto *et al.*, 2001). BGP has
480 been shown to be a highly significant protein in bony tissues in amphibians (Viegas *et*
481 *al.*, 2002), teleosts and sturgeon fishes (Bensimon-Brito *et al.*, 2012; Viegas *et al.*,
482 2013). The observed up-regulation of *bgp* from 10 dph onwards coincided with the start
483 of mineralization of dermal elements of the head and body surface during larval
484 development of *A. persicus*, which could be attributed to the role of BGP in
485 skeletogenesis. Increasing *bgp* mRNA expression in *A. persicus* is similar to that
486 observed in European sea bass (*Dicentrarchus labrax*) (Linnaeus, 1758) (Darias *et al.*,
487 2010), zebrafish (*Danio rerio*) (Hamilton, 1822) and Senegalese sole (*Solea*
488 *senegalensis* Kaup, 1858) (Gavaia *et al.*, 2006). This study is the first to examine mRNA
489 expression of the *mgp* gene during larval development of a Chondrostei species. The
490 least *mgp* transcript was observed during the endogenous feeding period, after which
491 *mgp* levels increased until 30 dph and then decreased at 50 dph, coinciding with
492 transition to the early juvenile stage. It has been previously found that MGP in sturgeons
493 is the most densely γ -carboxylated protein among known MGPs in vertebrates, with
494 seven Gla residues. This protein is known as a key regulator of chondral and
495 intramembranous ossification, and is a basic factor for differentiation and maturation of
496 chondrocytes (Viegas *et al.*, 2013). Recent studies have demonstrated the presence of
497 *mgp* transcripts in a wide variety of soft, cartilaginous and bony tissues in both
498 sturgeons (Viegas *et al.*, 2013) and modern teleosts such as Atlantic salmon (*Salmo*
499 *salar*) (Krossøy *et al.*, 2009) and turbot (*Scophthalmus maximus*) (Linnaeus, 1758)

500 (Roberto *et al.*, 2009). The considerable up-regulation of *mgp* transcripts from 20 dph
501 onwards, and particularly at 30 dph, in *A. persicus* could be related to the strong
502 mineralization of different dermal elements from the head and body surface, such as the
503 subopercle, supracleithrum, parietal, bony scutes from dorsal and ventral rows and the
504 anal, pelvic, dorsal and caudal fins and their respective pterygiophores. The increasing
505 trend in *mgp* transcript levels has also been observed in teleosts such as *D. rerio*, *S.*
506 *senegalensis* and *S. aurata*, where highest *mgp* expression levels were observed during
507 larval developmental phases coinciding with first feeding, metamorphosis and the end of
508 the larval stage, respectively (Gavaia *et al.*, 2006; Fernández *et al.*, 2011). The present
509 study also observed that *grp* mRNA levels increased during *A. persicus* development.
510 GRP plays a critical role in processes involving connective tissue mineralization, with
511 the highest number of Gla residues in all vertebrates; the Gla domain confer on these
512 proteins their ability to bind of calcium ions (Viegas *et al.*, 2013). Moreover, *grp* is most
513 highly expressed in cartilaginous tissues, especially mature and immature chondrocytes
514 of vertebra and in the upper and lower jaws, as well as in the chordoblast layer of the
515 notochord in sturgeons, which suggests a more widespread role for GRP throughout
516 skeletal formation (Viegas *et al.*, 2008).

517

518 **CONCLUSIONS**

519 Results of the present study showed that cartilage development in *A. persicus* started just
520 after hatching in the head and notochord. Initial mineralization processes seemed to
521 occur in the dentary, dermopalatine and palatopterygoid elements of the upper jaw,

522 coinciding with the onset of exogenous feeding. Genes encoding extracellular matrix
523 proteins (*bgp*, *mgp* and *grp*) were up-regulated during the exogenous feeding phase.
524 Strong mineralization of the skeletal elements occurring between 21.5 and 27.3 mm L_T
525 (20 dph) was in accordance with maximal levels of *bgp*, *mgp* and *grp* mRNA
526 expression, suggesting that genes encoding vitamin k-dependant proteins might be
527 correlated with mineralization of dermal tissues during sturgeon development. These
528 observations provide a reference for future studies seeking to evaluate larval quality and
529 the influence of biotic and abiotic rearing factors in the skeletogenesis of *A. persicus* and
530 the occurrence of skeletal deformities.

531

532 **Acknowledgments**

533 The authors would like to thank Shahid Beheshti Artificial Sturgeon Propagation and
534 Rearing Center for providing *A. persicus* samples, and Dr. R. Kazemi, Dr. Cerny and
535 Mr. M. Parashkoh for their helpful comments. Funding was provided by the research
536 deputy of University of Hormozgan (Iran).

537

538

539 **References**

540 Akbarzadeh, A., Farahmand, H., Mahjoubi, F., Nematollahi, M. A., Leskinen, P.,
541 Rytkönen, K. & Nikinmaa, M. (2011). The transcription of l-gulono-gamma-
542 lactone oxidase, a key enzyme for biosynthesis of ascorbate, during development

543 of Persian sturgeon (*Acipenser persicus*). *Comparative Biochemistry and*
544 *Physiology B* **158**, 282-288. <http://doi.org/10.1016/j.cbpb.2010.12.005>

545 Babaei, S. S., Kenari, A. A., Nazari, R. & Gisbert, E. (2011). Developmental changes of
546 digestive enzymes in Persian sturgeon (*Acipenser persicus*) during larval
547 ontogeny. *Aquaculture* **318**, 138-144. doi: 10.1016/j.aquaculture.2011.04.032

548 Bensimon-Brito, A., Cardeira, J., Cancela, M. L., Huysseune, A. & Witten, P. E. (2012).
549 Distinct patterns of notochord mineralization in zebrafish coincide with the
550 localization of Osteocalcin isoform 1 during early vertebral centra formation.
551 *BMC Developmental Biology* **12**, 28. doi: 10.1186/1471-213X-12-28

552 Bensimon-Brito, A., Cardeira, J., Dionísio, G., Huysseune, A., Cancela, M. L. & Witten,
553 P. E. (2016). Revisiting in vivo staining with alizarin red S-a valuable approach
554 to analyse zebrafish skeletal mineralization during development and
555 regeneration. *BMC Developmental Biology* **16**, 2. doi: 10.1186/s12861-016-
556 0102-4

557 Boglione, C., Gavaia, P., Koumoundouros, G., Gisbert, E., Moren, M., Fontagné, S.,
558 Witten, P. E. (2013a). Skeletal anomalies in reared European fish larvae and
559 juveniles. Part 1: normal and anomalous skeletogenic processes. *Reviews in*
560 *Aquaculture* **5**, S99-S120. doi: 10.1111/raq.12015

561 Boglione, C., Gisbert, E., Gavaia, P., Witten, P. E., Moren, M., Fontagné, S. &
562 Koumoundouros, G. (2013b). Skeletal anomalies in reared European fish larvae
563 and juveniles. Part 2: main typologies, occurrences and causative factors.
564 *Reviews in Aquaculture* **5**, S121-S167. doi: 10.1111/raq.12016

- 565 Boskey, A., Gadaleta, S., Gundberg, C., Doty, S., Ducey, P. & Karsenty, G. (1998).
566 Fourier transform infrared microspectroscopic analysis of bones of osteocalcin-
567 deficient mice provides insight into the function of osteocalcin. *Bone* **23**, 187-
568 196. [http://doi.org/10.1016/S8756-3282\(98\)00092-1](http://doi.org/10.1016/S8756-3282(98)00092-1)
- 569 Bronzi, P., Rosenthal, H. & Gessner, J. (2011). Global sturgeon aquaculture production:
570 an overview. *Journal of Applied Ichthyology* **27**, 169-175. doi: 10.1111/j.1439-
571 0426.2011.01757.x
- 572 Cancela, M. L., Conceição, N. & Laizé, V. (2012). Gla-rich protein, a new player in
573 tissue calcification? *Advances in Nutrition* **3**, 174-181.
574 doi:10.3945/an.111.001685
- 575 Darias, M., Lan Chow Wing, O., Cahu, C., Zambonino-Infante, J. & Mazurais, D.
576 (2010). Double staining protocol for developing European sea bass
577 (*Dicentrarchus labrax*) larvae. *Journal of Applied Ichthyology* **26**, 280-285. doi:
578 10.1111/j.1439-0426.2010.01421.x
- 579 Dettlaff, T. A., Ginsburg, A. S. & Schmalhausen, O. I. (1993). Sturgeon fishes.
580 Developmental biology and aquaculture. Springer-Verlag, Berlin. pp. 300.
- 581 Dourado-Villa, J. K., Diaz, M. A. N., Pizziolo, V. R. & Martino, H. S. D. (2017). Effect
582 of vitamin K in bone metabolism and vascular calcification: a review of
583 mechanisms of action and evidences. *Critical Reviews in Food Science and*
584 *Nutrition*, in press. <http://dx.doi.org/10.1080/10408398.2016.1211616>

- 585 Eshaghzadeh, H., Alcaraz, C., Akbarzadeh, A. & Gisbert, E. (2017). The combination of
586 bivariate and multivariate methods to analyze character synchronization and
587 early allometric growth patterns in the stellate sturgeon (*Acipenser stellatus*
588 Pallas, 1771) as tools for better understanding larval behavior. *Canadian Journal*
589 *of Fisheries and Aquatic Sciences*, in press. doi: 10.1139/cjfas-2016-0288
- 590 Fernández, I., Darias M., Andree K B., Mazurais D., Zambonino-Infante J. L. & Gisbert
591 E. (2011). Coordinated gene expression during gilthead sea bream skeletogenesis
592 and its disruption by nutritional hypervitaminosis A. *BMC Developmental*
593 *Biology* **11**, 1-7. doi: 10.1186/1471-213X-11-7
- 594 Findeis, E. K. (1997). Osteology and phylogenetic interrelationships of sturgeons
595 (Acipenseridae). *Environmental Biology of Fishes* **48**, 73-126. doi:
596 10.1023/A:1007372832213
- 597 Gavaia, P. J., Sarasquete, C. & Cancela, M. L. (2000). Detection of mineralized
598 structures in early stages of development of marine Teleostei using a modified
599 alcian blue-alizarin red double staining technique for bone and cartilage.
600 *Biotechnic & Histochemistry* **75**, 79-84. doi:
601 <http://dx.doi.org/10.3109/10520290009064151>
- 602 Gavaia, P. J., Simes, D. C., Ortiz-Delgado, J., Viegas, C. S., Pinto, J. P., Kelsh, R. N.,
603 Sarasquete, M. C. & Cancela M. L. (2006). Osteocalcin and matrix Gla protein
604 in zebrafish (*Danio rerio*) and Senegal *S. senegalensis*: Comparative gene and
605 protein expression during larval development through adulthood. *Gene*
606 *Expression Patterns* **6**, 637-652. <http://doi.org/10.1016/j.modgep.2005.11.010>

- 607 Gisbert, E. (1999). Early development and allometric growth patterns in Siberian
608 sturgeon and their ecological significance. *Journal Fish Biology* **54**, 852-862.
609 doi: 10.1111/j.1095-8649.1999.tb0203
- 610 Gisbert, E. & Doroshov, S. I. (2003). Histology of the developing digestive system and
611 the effect of food deprivation in larval green sturgeon (*Acipenser medirostris*).
612 *Aquatic Living Resources* **16**, 77-89. <https://doi.org/10.1016/S0990-7440>
613 (03)00029-9
- 614 Gisbert, E. & Doroshov, S. I. (2006). Allometric growth in green sturgeon larvae.
615 *Journal of Applied Ichthyology* **22**, 202–207. doi: 10.1111/j.1439-
616 0426.2007.00952.x
- 617 Gisbert, E., Asgari, R., Rafiee, G., Agh, N., Eagderi, S., Eshaghzadeh, H. & Alcaraz, C.
618 (2014). Early development and allometric growth patterns of beluga *Huso huso*
619 (Linnaeus, 1758). *Journal of Applied Ichthyology* **30**, 1264-1272. doi:
620 10.1111/jai.12617
- 621 Gluckmann, I., Huriaux, F., Focant, B. & Vandewalle, P. (1999). Postembryonic
622 development of the cephalic skeleton in *Dicentrarchus labrax* (Pisces,
623 Perciformes, Serranidae). *Bulletin of Marine Science* **65**: 11-36.
- 624 Grande, L., & Hilton, E. J. (2006). An exquisitely preserved skeleton representing a
625 primitive sturgeon from the Upper Cretaceous Judith River Formation of
626 Montana (Acipenseriformes: Acipenseridae: n. gen. and sp). *Journal of*
627 *Paleontology* **80**, 1-39. <http://dx.doi.org/10.1666/05032.1>

- 628 Hanken, J. & Wassersug, R. (1981). The visible skeleton. *Functional Photography* **16**,
629 22-26.
- 630 Hilton, E. J. (2005). Observations on the skulls of sturgeons (Acipenseridae): Shared
631 similarities of *Pseudoscaphirhynchus kaufmanni* and juvenile specimens of
632 *Acipenser stellatus*. *Environmental Biology of Fishes* **72**, 135-144. doi:
633 10.1007/s10641-004-6578-y
- 634 Hilton, E. J., Grande, L. & Bemis, W. E. (2011). Skeletal anatomy of the shortnose
635 sturgeon, *Acipenser brevirostrum* Lesueur, 1818, and the systematics of
636 sturgeons (Acipenseriformes, Acipenseridae). *Fieldiana Life and Earth Sciences*
637 **3**, 1-168.
- 638 Jollie, M. (1980). Development of head and pectoral girdle skeleton and scales in
639 *Acipenser*. *Copeia* **1980**, 226-249.
- 640 Khajepour, F. & Hosseini, S. A. (2010). Mineral status of juvenile beluga (*Huso huso*)
641 fed citric acid supplemented diets. *World Applied Sciences Journal* **11**, 682-686.
- 642 Krossøy, C., Ørnstrud, R. & Wargelius, A. (2009). Differential gene expression of bgp
643 and mgp in trabecular and compact bone of Atlantic salmon (*Salmo salar* L.)
644 vertebrae. *Journal of Anatomy* **215**, 663-672. doi: 10.1111/j.1469-
645 7580.2009.01153.x
- 646 Leprévost, A. & Sire, J. Y. (2014). Architecture, mineralization and development of the
647 axial skeleton in Acipenseriformes, and occurrences of axial anomalies in rearing

648 conditions; can current knowledge in teleost fish help? *Journal of Applied*
649 *Ichthyology* **30**, 767-776. doi: 10.1111/jai.12525

650 Livak, K. J. & Schmittgen, T. D. (2001). Analysis of Relative Gene Expression Data
651 Using Real-Time Quantitative PCR and the 2- $\Delta\Delta$ CT method. *Methods* **25**, 402-
652 408. <https://doi.org/10.1006/meth.2001.1262>

653 Luo G., Ducey P., McKee M. D., Pinero G. J., Loyer E., Behringer R. R. & Karsenty G.
654 (1997). Spontaneous calcification of arteries and cartilage in mice lacking matrix
655 GLA protein. *Nature* **386**, 78-81. doi:10.1038/386078a0Osse, J. & Van den
656 Boogaart, J. (1995). Fish larvae, development, allometric growth, and the aquatic
657 environment. *ICES Marine Science Symposia* **201**, 21–34.

658 Near, T. J., Eytan, R. I., Dornburg, A., Kuhn, K. L., Moore, J. A., Davis, M. P. & Smith,
659 W. L. (2012). Resolution of ray-finned fish phylogeny and timing of
660 diversification. *Proceedings of the National Academy of Sciences of the United*
661 *States of America* **109**, 13698–13703. <http://doi.org/10.1073/pnas.1206625109>

662 Park, C., Lee, S. Y., Kim, D. S. & Nam, Y. K. (2013). Effects of incubation temperature
663 on egg development, hatching and pigment plug evacuation in farmed Siberian
664 sturgeon *Acipenser baerii*. *Fisheries and Aquatic Sciences* **16**, 25-34. doi:
665 10.5657/FAS.2013.0025

666 Pinto, J., Ohresser, M. & Cancela, M. (2001). Cloning of the bone Gla protein gene
667 from the teleost fish (*Sparus aurata*). Evidence for overall conservation in gene
668 organization and bone-specific expression from fish to man. *Gene* **270**, 77-91.
669 [http://doi.org/10.1016/S0378-1119\(01\)00426-7](http://doi.org/10.1016/S0378-1119(01)00426-7)

670 Roberto, V. P., Cavaco, S., Viegas, C. S., Simes, D. C., Ortiz-Delgado, J. B.,
671 Sarasquete, M. C., Gavaia, P. J. & Cancela, M. L. (2009). Matrix Gla protein in
672 turbot (*Scophthalmus maximus*): Gene expression analysis and identification of
673 sites of protein accumulation. *Aquaculture* **294**, 202-211.
674 <http://doi.org/10.1016/j.aquaculture.2009.06.020>

675 Sfakianakis, D., Koumoundouros, G., Divanach, P. & Kentouri, M. (2004). Osteological
676 development of the vertebral column and of the fins in (*Pagellus erythrinus* L.
677 1758). Temperature effect on the developmental plasticity and morpho-
678 anatomical abnormalities. *Aquaculture* **232**, 407-
679 424.<https://doi.org/10.1016/j.aquaculture.2003.08.014>

680 Vermeer, C. (1990). Gamma-carboxyglutamate-containing proteins and the vitamin K-
681 dependent carboxylase. *Biochemical Journal* **266**, 625-636.

682 Viegas, C., Pinto, J., Conceicao, N., Simes, D. & Cancela, M. (2002). Cloning and
683 characterization of the cDNA and gene encoding *Xenopus laevis* osteocalcin.
684 *Gene* **289**, 97-107. [http://doi.org/10.1016/S0378-1119\(02\)00480-8](http://doi.org/10.1016/S0378-1119(02)00480-8)

685 Viegas, C., S. Simes, D. C., Laizé, V., Williamson, M. K., Price, P. A. & Cancela, M. L.
686 (2008). Gla-rich protein (GRP), a new vitamin K-dependent protein identified
687 from sturgeon cartilage and highly conserved in vertebrates. *Journal of*
688 *Biological Chemistry* **283**, 36655-36664. doi: 10.1074/jbc.M802761200

689 Viegas, C. S., Simes, D. C., Williamson, M. K., Cavaco, S., Laizé, V., Price, P. A. &
690 Cancela, M. L. (2013). Sturgeon osteocalcin shares structural features with
691 matrix Gla protein: evolutionary relationship and functional implications.

692 *Journal of Biological Chemistry* **288**, 27801-27811. doi:
693 10.1074/jbc.M113.450213

694 Wagemans, F. & Vandewalle, P. (2001). Development of the bony skull in common
695 sole: brief survey of morpho-functional aspects of ossification sequence. *Journal*
696 *of Fish Biology* **59**, 1350-1369. doi: 10.1111/j.1095-8649.2001.tb00197.x

697 Walker, M. B. & Kimmel, C. B. (2007). A two-color acid-free cartilage and bone stain
698 for zebrafish larvae. *Biotechnic & Histochemistry* **82**, 23-28.
699 <http://dx.doi.org/10.1080/10520290701333558>

700 Wang, S., Furmanek, T., Kryvi, H., Krossøy, C., Totland, G. K., Grotmol, S. &
701 Wargelius, A. (2014). Transcriptome sequencing of Atlantic salmon (*Salmo*
702 *salar* L.) notochord prior to development of the vertebrae provides clues to
703 regulation of positional fate, chordoblast lineage and mineralisation. *BMC*
704 *Genomics* **15**, 141. doi: 10.1186/1471-2164-15-141

705 Wilga, C. & Lauder, G. (1999). Locomotion in sturgeon: function of the pectoral fins.
706 *Journal of Experimental Biology* **202**, 2413-2432.

707 Zhang, X., Shimoda, K., Ura, K., Adachi, S. & Takagi Y. (2012). Developmental
708 structure of the vertebral column, fins, scutes and scales in bester sturgeon, a
709 hybrid of beluga *Huso huso* and sterlet *Acipenser ruthenus*. *Journal of Fish*
710 *Biology* **81**, 1985-2004. doi: 10.1111/j.1095-8649.2012.03451.x

711

712 Table1. Candidate reference and target genes tested for quantitative real-time PCR in

713 *Acipenser persicus*.

Genes	Primers, Forward/Reverse	Amplicon size
Bone Gla protein	F- TCTGACGCTGTTTTGCTCCAGTAAATCTCG R- CGTTTCAGGGAAAATACCCAAAAGCAATA	95
Matrix Gla protein	F- CTGGCTACTACTATGAGAGGTTAATGG R- GGTCACATGGGGTGTGCT	135
Gla Rich protein	F- TGTAGAGGAGGAGCGTGATGAGCAGCA R- CATGATGTCCTTTTTTGGCGATTGTGTTC	163
beta-actin	F- TGGAGGTACCACCATGTACCC R- CACATCTGCTGGAAGGTGGA	167
Ribosomal protein L6	F- GTGGTCAAACCTCCGCAAGA R- GCCAGTAAGGAGGATGAGGA	149

714

715

716

Figure captions

717 **Fig. 1.** Skeletogenesis of *Acipenser persicus* from hatching (10.9 mm L_T) to 50 days
718 post hatching (dph) (48.4 mm L_T). a) Hatching time, b) 1 dph, c) 3 dph, d) 6 dph, e) 10
719 dph, f) 12 dph, g) 14 dph, h) 20 dph, i) 30 dph, j) 50 dph (acidic staining) and k) 50 dph
720 (non-acidic staining). *Abbreviations:* a= anus, br = branchiostegal, cha = anterior
721 ceratohyal, chp = posterior ceratohyal, cl = cleithrum, clv = clavicle, dpt =
722 dermopterotic, dr = distal radial, ds = dorsal scute, dsp = dermosphenotic, h= hyoid
723 arch, hyp = hypural, ihy = interhyal, j = jugal, lrb = lateral rostral canal bone, m =
724 melanin plug, mc = Meckel's cartilage, mr = middle radial, n = notochord, pa=
725 palatoquadrates, pas = parasphenoid, pat = pars autopalatina, pf = primordial finfold,
726 phy= parhypural, po = postorbital, pp = pelvic pterygiophore, pr= proximal radial, pt =
727 posttemporal, rcb = rostral canal bones, scl = supracleithrum, so = supraorbital, sp=
728 spiral valve (scale bar = 1 mm).

729

730 **Fig. 2.** Ventral and dorsal views of the head of *Acipenser persicus* showing the
731 mineralization of different skeletal elements during larval development [19.9 - 48.5 mm
732 L_T , 10 days post hatching (dph) to 50 dph]. a) Unmineralized teeth in both jaws at 10
733 dph; b) ventral view of the jaw at early stages of development (12 dph); c) weak
734 mineralized dermal bones of head and dorsal scutes at 20 dph; d) ventral view of
735 branchial arch at 10 dph, e) Strong mineralization of dermal bones in dorsal view of head;
736 f & g) ventral view of hyoid arch at 50dph. *Abbreviations:* bbc = basibranchial copulae,
737 cb = ceratobranchial, cha = anterior ceratohyal, chp = posterior ceratohyal, d = dentary,

738 dpl = dermopalatin, dpt = dermopterotic, drb = dorsal rostral bone, dsp =
739 dermosphenotic, excm = median extrascapular, fr = frontal, h = hyomandibula, hb =
740 hypobranchial, hh = hypohyal, ihy = interhyal, j = jugal, lrb = lateral rostral canal bone,
741 pa = parietal, pt = posttemporal, rcb = rostral canal bones, scl = supracleithrum, sop =
742 subopercle, t = teeth, vrb = ventral rostral bone (scale bar 1mm).

743

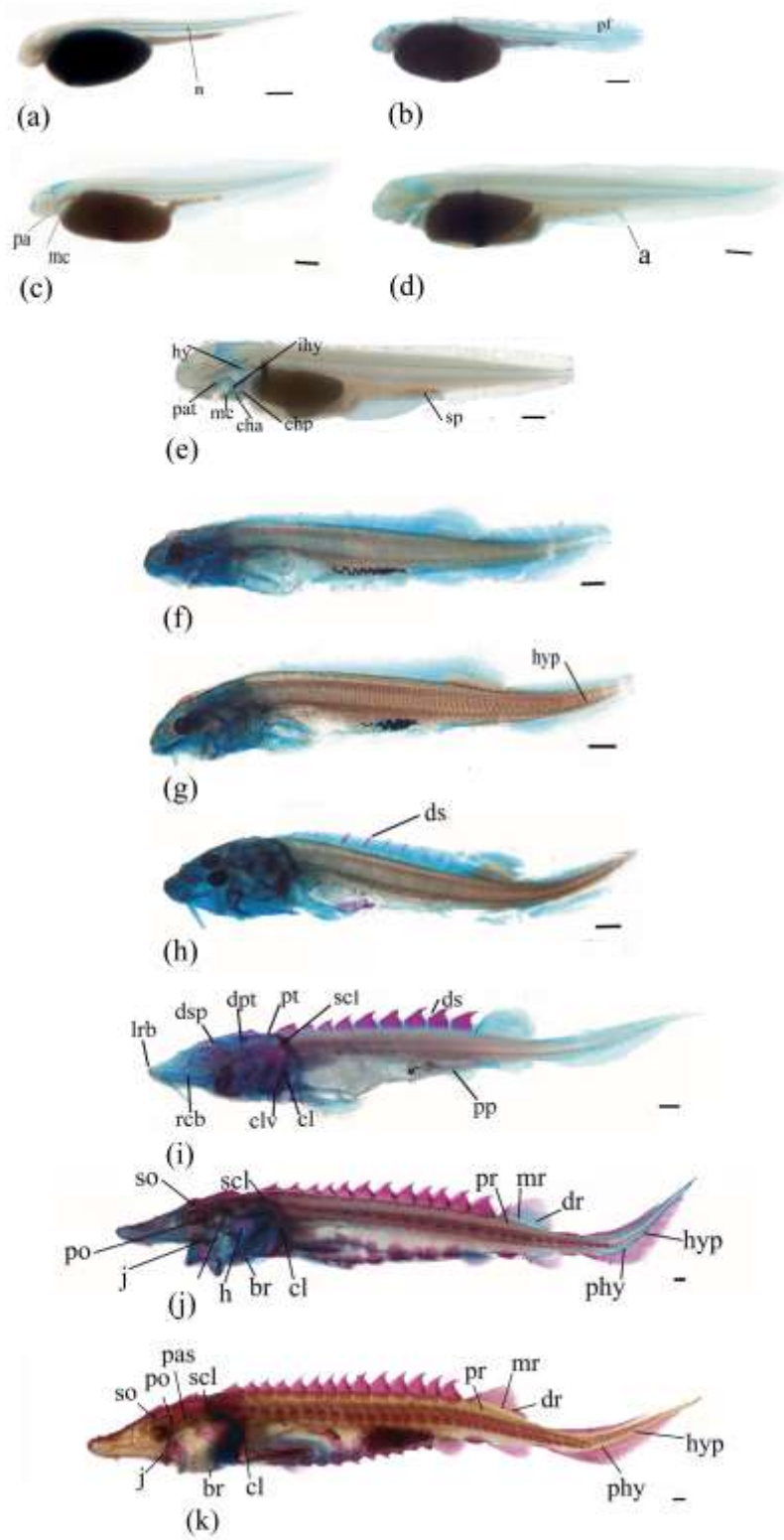
744 **Fig. 3.** Log₂ expression of the (a) *bgp*, (b) *mgp* and (c) *grp* genes during the
745 development of *Acipenser persicus* from 1 day post hatching (dph) to 50 dph. The
746 values are considered as mean ± SD (n = 3). Statistical significance of differences of the
747 normalized *bgp*, *mgp* and *grp* data between samples taken at different developmental
748 times was analyzed using one-way ANOVA followed by Tukey's multiple-comparison
749 test. Bars with different letters are significantly different ($P < 0.05$).

750

751

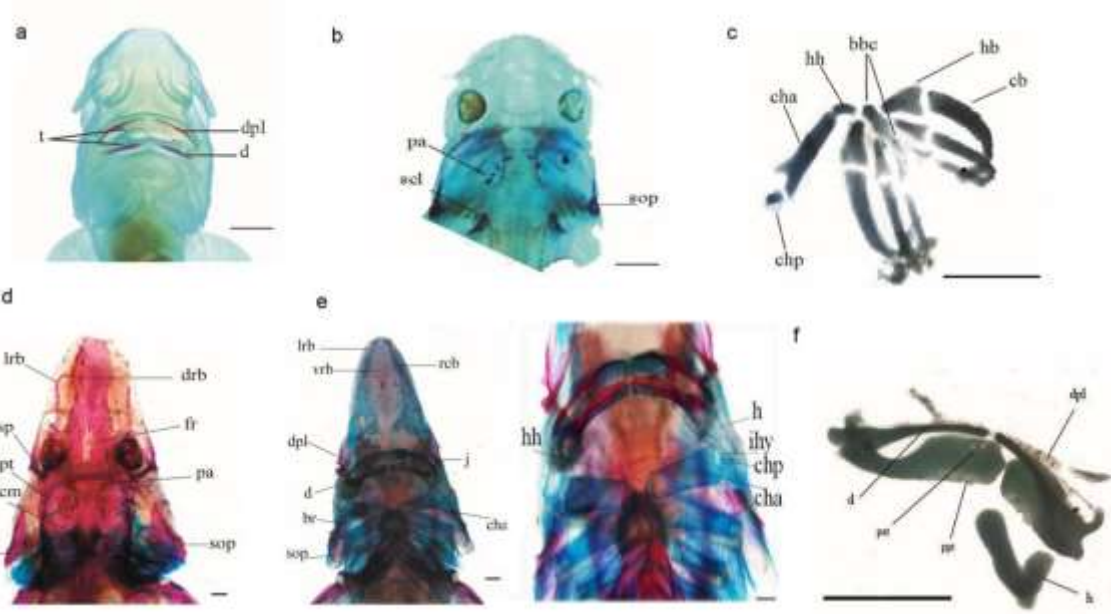
752

753 Figure 1.



754

755 Figure 2

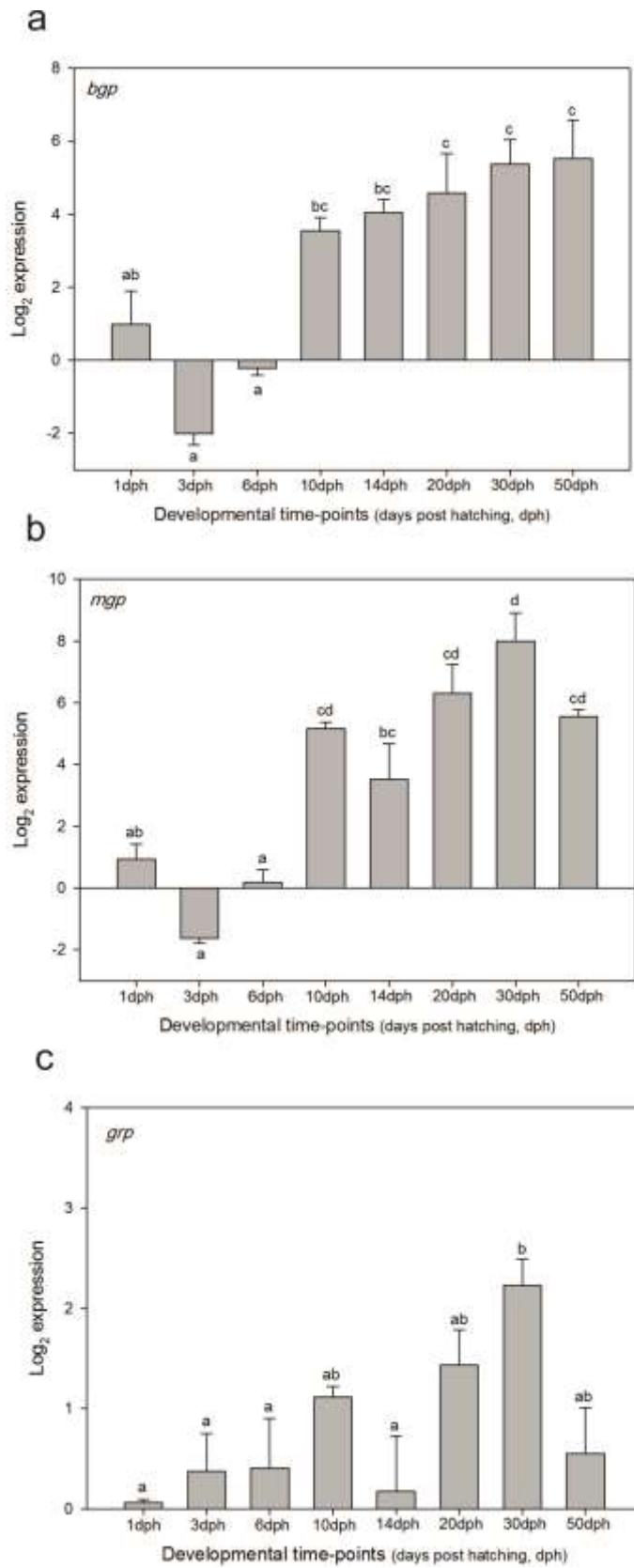


756

757

758

759 Figure 3



760

761

762

763

764